Polymer chains confined into tubes with attractive walls: A Monte Carlo simulation

Andrey Milchev[a], *Wolfgang Paul, Kurt Binder**

Institut für Physik, Johannes-Gutenberg-Universität Mainz,
Staudinger Weg 7, D-55099 Mainz, Germany

(Received: June 2, 1993; revised manuscript of July 9, 1993)

SUMMARY:

A bead-spring off-lattice model of a polymer chain with repulsive interactions among repeating units confined into straight tubes of various cross sections, D_T^2, is studied by Monte Carlo simulation. We are also varying the chain length from $N = 16$ to 128 and the strength of a short-range attractive interaction between the repeating units and the walls of the tube. Longitudinal and perpendicular static linear dimensions of the chains are analyzed, as well as the density profile of repeating units across the tube. These data are interpreted in terms of scaling concepts describing the crossover between three-dimensional and quasi-one-dimensional chain conformations and the adsorption transition of chains at flat infinite walls, respectively. We also study the time-dependent mean-square displacements of repeating units and obtain various relaxation times. It is shown that both relaxation times scaling proportional to N^2 and to N^3 play a role in the reptative motion of the chain in these tubes.

1. Introduction

The properties of flexible polymer chains moving in porous structures are relevant for applications such as filtration, gel permeation chromatography, oil recovery etc.[1,2] This is also an exciting problem of statistical physics, since the conformation of the macromolecule in such a tube in a porous material may be very severely distorted in comparison to the conformations that the polymer takes in bulk solution. This distortion of the polymer geometry may have two rather different sources: if the cross section D_T^2 of the narrow tube in which the polymer moves is smaller than the mean-square radius of gyration $\langle R_{gyr}^2 \rangle_{bulk}$ that the polymer takes in bulk solution, there is a purely geometric constraining effect due to the excluded-volume interaction between the repeating units of the polymer and the walls of the tube. As a result, one expects the random coil in a straight tube to be deformed into a long cigar-shaped object, such that $\langle R_{gyr,\perp}^2 \rangle$ is of order D_T^2 and hence fits into the tube, while $\langle R_{gyr,\parallel}^2 \rangle$ now is much larger than the bulk radius square, $\langle R_{gyr}^2 \rangle_{bulk}$. The resulting crossover of the polymer coil conformation from three-dimensional to quasi-one-dimensional has been studied both by scaling considerations[1,3] and simulations[3,4]. The second reason for a distortion of the polymer conformation is that in many cases there will also be an attractive interaction between the repeating units and the walls of the tube. While much work was devoted to the adsorption of polymers from solutions to planar walls in semi-infinite geometry (e.g. refs.[4–10]), we are not aware of related studies of adsorbing tubes. While for a purely repulsive excluded-volume interaction between repeating units

[a] Present and permanent address: Institute of Physical Chemistry, Bulgarian Academy of Sciences, 1040 Sofia, Bulgaria.

 CCC 1022-1344/94/$03.00

and the walls it is most favorable for the chain — from the point of view of configurational entropy — to stay off the walls as much as possible, the attractive interaction which likes to adsorb the units at the wall may balance or overrule this tendency. Obviously, we thus have to expect a delicate competition between entropic forces — which want to localize the chain in the center of the tube, away from the walls — and the enthalpic forces, which try the contrary. A first exploration of these interesting effects is the aim of the present paper. Particularly interesting are also the consequences of this behavior on dynamic properties of the chains, since most applications mentioned above involve transport of the polymers through the porous medium, and motions of chains in constrained geometries pose interesting theoretical problems, such as exemplifying reptation [11–14], anomalous diffusion [15], entropic traps [16, 17] etc.

In the next section we now define the off-lattice model of polymers that is studied by Monte Carlo simulations here. In a previous work [18] the bulk properties of this model in dilute and concentrated solutions have been exhaustively studied. Since the equilibrium of long polymer chains in computer simulations is a delicate problem [19, 20], it is necessary to choose both the coarse-grained polymer model and the constraining geometry such that a very efficient Monte Carlo algorithm becomes feasible. Sec. 3 presents then the average geometric characteristics of the chains (longitudinal and transverse components of the squared gyration radius), and studies them as function of three parameters: tube cross section, chain length and strength of the attractive interaction between repeating units and the wall. Wherever possible we compare the data to theoretical predictions [1, 3, 5, 21, 22]. Sec. 4 presents data on the monomer density profiles across the tube. Evidence for a transition from non-adsorbed chains (localized in the center of the tube) to adsorbed chains (localized at the walls of the tube) is presented. Sec. 5 describes some results on mean-square displacements of the repeating unit as function of time, both for longitudinal and transverse motions. Various relaxation times are extracted and compared to predictions due to reptation theory. Sec. 6 then summarizes our conclusions.

2. The polymer model and the pore geometry

For a conclusive test of the theoretical ideas sketched in the introduction one needs a polymer model that can be simulated very efficiently. Therefore, first simulations on this problem have used a lattice model, representing the chain as a self-avoiding walk on the diamond lattice [3]. However, for chains in narrow tubes such a lattice model has also disadvantages: large parts of the chain can be temporarily locked in and cannot move at all until their environment has relaxed. There are also problems of principle since almost always the algorithms are not strictly ergodic [23, 24].

Variations of the model (such as variable degree of chain stiffness, etc.) are often difficult to introduce, at least if one does not wish to sacrifice most of the program efficiency. Thus in the present work we use an off-lattice model of bead-spring type. The effective monomeric units along the chain are coupled by a restricted harmonic potential for the length of the bond between them

$$U(l) = k \cdot (l - l_0)^2 \quad \text{for} \quad l_{\min} < l < l_{\max} \tag{1}$$

$$U(l) = \infty \quad \text{for} \quad l \le l_{\min} \quad \text{or} \quad l \ge l_{\max} \tag{2}$$

Choosing $l_{\max} = 1$ as the unit of length, we use [18] $l_0 = 0{,}7$, $l_{\min} = 0{,}4$. We choose the spring constant k in Eq. (1) rather stiff (by working at a temperature T such that $k/(k_B \cdot T) = 10$), so that the cutoff at $l_{\min}$ and $l_{\max}$ has little effect on the configurations of the chains [18]. As a non-bonded interaction, we use the repulsive part of the Lennard-Jones-Potential [18],

$$V(r) = 4\varepsilon_{LJ}\{[(\sigma_{LJ}/r)^{12} - (\sigma_{LJ}/r)^6] + 1\} \quad \text{for} \quad r < 2^{1/6}\sigma_{LJ} \tag{3}$$

$$V(r) = 0 \quad \text{for} \quad r > 2^{1/6}\sigma_{LJ} \tag{4}$$

Here the range parameter σ_{LJ} is chosen such that the cutoff coincides with $l_{\max}$, $2^{1/6}\sigma_{LJ} = 1$, and the strength parameter ε_{LJ} is chosen weak (in comparison with temperature), $k_B \cdot T/\varepsilon_{LJ} = 10$, so only the steeply varying part of $V(r)$ and not the region near the cutoff matters. With respect to bulk static and dynamic properties of polymer chains described by this model, previous work [18] has shown that asymptotic properties are already reached for rather small chain length N, and a reasonable description of the crossover from dilute to concentrated solutions (compatible with related work on lattice models [25]) did emerge. The Monte Carlo algorithm (where repeating units attempt to jump to a randomly chosen position in a cube of unit length centered around their old position) has a reasonably large acceptance rate (these rather large moves are typically accepted with probability of order 0,1) and allows to use the link-cell method, as discussed below. In view of these properties, this model was found to be nearly as efficient as comparable highly optimized lattice codes [25].

For an efficient performance of off-lattice Monte Carlo simulations of polymer chains the use of the link-cell scheme is absolutely crucial, as lots of unnecessary computation of distances to other repeating units are avoided. For the present application, it was very desirable to preserve the features of this link-cell scheme as much as possible. For this reason of computational efficiency we work with a straight tube of square rather than circular cross section (Fig. 1). While at first sight this may look rather artificial, we argue that both ideal straight tubes with square cross section and with circular cross section are similarly artificial: in real porous materials, tubes are not straight but contorted, their cross section fluctuates both in size and in shape, and special effects may occur near the bifurcation points of the pore network [16]. The real tubes thus bring in one more qualitatively important feature of porous materials, that is deliberately omitted here, namely "frozen in" statistical disorder. Here we intentionally wish to eliminate many such aspects of real tubes in porous media, in order to be able to bring out clearly two aspects which we feel are relevant for more complicated problems, too: first of all, the chain confinement of the polymers moving in a quasi-one-dimensional geometry, and secondly, the modification of chain structure and dynamics due to the attractive interactions with the wall. Both aspects are included in our model in a very simple way. As an illustration, a snapshot picture of such a confined chain is displayed in Fig. 2. We also note that more ideal narrow tubes occur in zeolithe crystals or other inclusion compounds [26] — but there, of

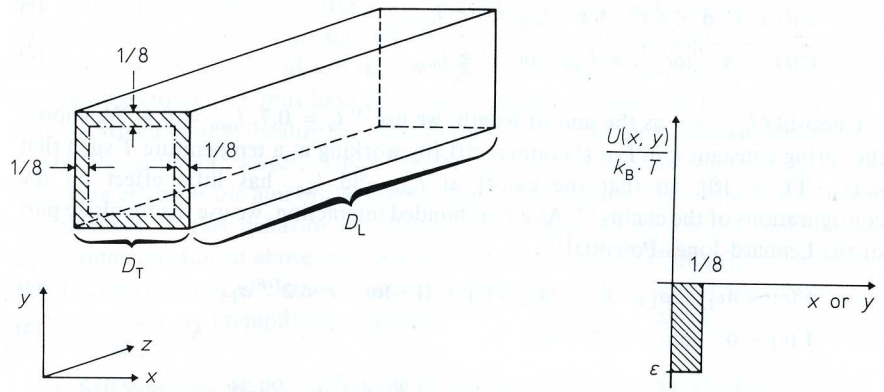

Fig. 1. Sketch of the tube geometry used: the cross section of the tube is a square of linear dimension D_T, oriented along the x and y axis, respectively. The linear dimension of the tube in z direction is D_L (and periodic boundary conditions in z direction are used). At the walls of the tube an attractive potential $U(x, y)$ acts, which is chosen as $U(x, y) = \varepsilon$ if $x < 1/8$ or $y < 1/8$ while otherwise $U(x, y) = 0$

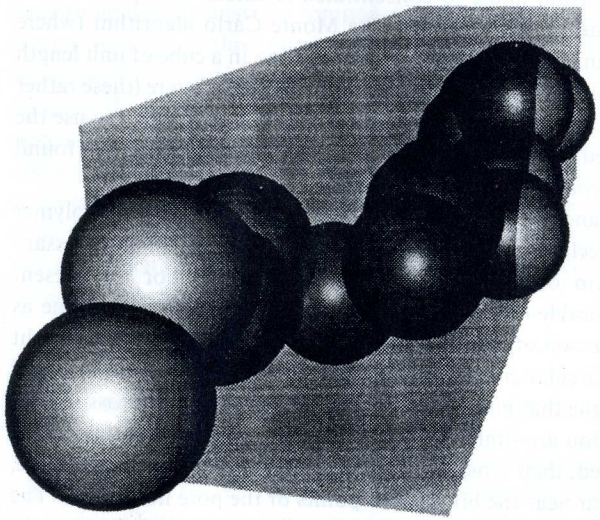

Fig. 2. Snapshot picture of a chain with $N = 16$ repeating units confined in a tube with $D_T = 4$ for $\varepsilon/(k_B \cdot T) = 0$. A sphere with radius $r = 0{,}4$ is drawn around each repeating unit (note that the center of gravity of each unit can come arbitrarily close to the walls, and therefore the spheres can intersect the walls although the units — at the center of the spheres — can never cross the walls)

course, the precise geometry of the wall reflects the crystal symmetry and one also must use a "corrugation potential" (periodic in z-direction along the tube) to reflect the crystal structure rather than the structureless potentials used here that do not depend on z. Of course, our study can be viewed as a first step that can be extended later into all these directions in an attempt to model materials and their properties in a more specific way, but at the moment the effect of such complications is disregarded.

The technical details of our simulations are as follows. We use tube linear dimensions $D_T = 1$, 2, and 4 (remember that $l_{max} = 1$ is our unit of length) and $D_L = 64$ and 128

(two choices for D_L have been studied only for the sake of verifying that the dependence of our results on D_L can be neglected — indeed we are interested only in the limiting behavior of $D_L \to \infty$). We use periodic boundary conditions in z-direction. The chain lengths considered are $N = 16$, 32, 64 and 128, while wall energies studied were $\varepsilon' = \varepsilon/(k_B \cdot T) = 0$, $-0{,}5$, -1, -2 and -3. Data for $N \leq 64$ have always been taken for $D_L = 64$ only, while data for $N = 128$ were taken for both choices of D_L. Unlike ref. [3] — where for a self-avoiding walk model tube diameters up to $D_T = 32$ lattice spacings were studied and chain length up to $N = 800$ — our interest here is not so much to establish what happens in the scaling limit ($D_T \to \infty$, $N \to \infty$ taken together in the suitably scaled combination) but rather to provide qualitative insight into the behaviour of chains in very narrow tubes as they are presumably prevailing in many materials.

For gaining statistics, many runs under otherwise identical conditions were taken and averaged over. This number of runs ranged from $n = 240$ (for $N = 16$) to $n = 100$ (for $N \geq 64$). Since these runs can be considered as statistically independent, they allow a straightforward estimation of statistical errors of the various quantities of interest. However, in the figures to follow statistical errors are not shown since in many figures (particularly on static radii) they are smaller than the size of the symbols, while in other figures (like the density histograms) they would confuse the picture and can be estimated from the fluctuations seen in these plots.

3. Linear dimension of chains in tubes with variable strength of wall attraction

As is standard [3] we consider longitudinal (denoted by index l) and transverse (t) components of the mean-square end-to-end distance $\langle R^2 \rangle$ and gyration radius $\langle R_g^2 \rangle$, respectively.

$$\langle R_{gl}^2 \rangle = \frac{1}{N} \sum_{i=1}^{N} \langle [z_i - z_{cm}]^2 \rangle$$

$$\langle R_{gt}^2 \rangle = \frac{1}{N} \sum_{i=1}^{N} \langle [x_i - x_{cm}]^2 + [y_i - y_{cm}]^2 \rangle \qquad (5)$$

the center of mass vector being denoted as $\boldsymbol{R}_{cm} = (x_{cm}, y_{cm}, z_{cm})$. Fig. 3 shows a log-log plot of $\langle R_{gl}^2 \rangle / N^{2\nu} \sim N^{2(1-\nu)} \approx N^{0{,}82}$, using $\nu \approx 0{,}59$ [12]. Apart from the case $D_T = 4$, $\varepsilon' = -2$, a slope of 0,83 is found, irrespective of D_T and ε', which is in excellent agreement with the theoretical prediction. Thus while the precise value of D_T and interaction strength ε' affect the prefactor in the relation $\sqrt{\langle R_{gl}^2 \rangle} \sim N$, the exponent of the power law is universal and does not depend on such "details" of the model (or on details of a real material, of course). This is once more an example for the usefulness of scaling ideas for polymers [12]. However, one cannot push all scaling concepts too far: while the scaling theory for $D_T \to \infty$ predicts [1, 3]

$$\langle R_{gl}^2 \rangle / N^{2\nu} = f(D_T / N^{\nu}) \quad \text{with} \quad f(x \ll 1) \sim x^{2-2/\nu} \approx x^{-1{,}4} \qquad (6)$$

it is seen that data for $D_T = 1$, 2 and 4 do not yet scale in this form (Fig. 4). In particular, the data points for $D_T = 1$ are quite off, but this must be expected since

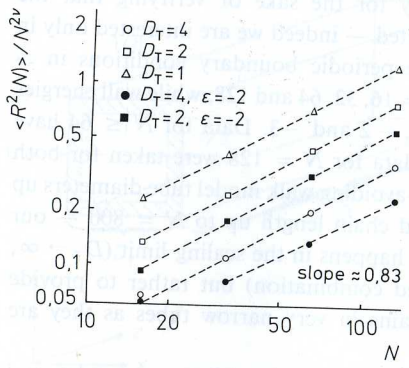

Fig. 3.

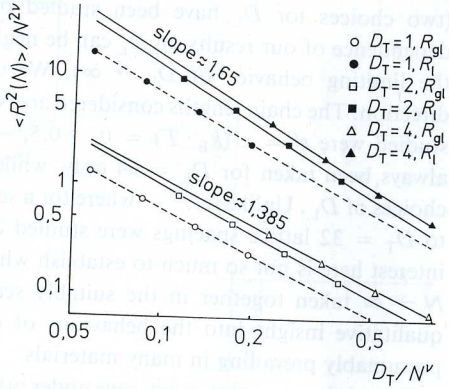

Fig. 4.

Fig. 3. Log-log plot of $\langle R_{gl}^2\rangle/N^{2\nu}$ versus N for several choices of D_T and ε' ($\varepsilon' = 0$ if not otherwise indicated). The four upper dashed straight lines have all the same slope of about 0,83

Fig. 4. Scaling plot of $\langle R_{gl}^2\rangle/N^{2\nu}$ (open symbols) and $\langle R_l^2\rangle/N^{2\nu}$ (full symbols) versus D_T/N^{ν}, for $\varepsilon' = 0$

now the tube linear dimension is of the same order as the bond length, and thus scaling must break down. The exponent predicted in Eq. (6) is roughly seen already for the gyration radius, although it is not seen for the end-to-end distance. But we expect that both quantities would scale for D_T of order 10, as for the lattice model in ref. [3] Even from the present work on very narrow tubes one can already roughly estimate the limiting behavior of very wide tubes from the scaling plot, inspired by Eq. (6).

Fig. 5 shows the transverse part of the gyration radius and thereby elucidates the role of the attractive wall interaction: while for $\varepsilon' = 0$ the chain wants to stay off the walls and this implies all repeating units must be close to the center of the tube, for $\varepsilon' < 0$ the monomers tend to be adsorbed on the walls and therefore $\langle R_{gt}^2\rangle$ is distinctly larger.

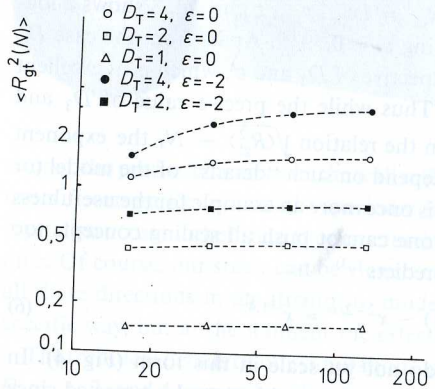

Fig. 5. Log-log plot of $\langle R_{gt}^2\rangle$ vs. N for several choices of D_T and ε', as indicated in the figure

It is also remarkable that much larger values of N are then needed to reach the saturation values of $\langle R_{gt}^2\rangle$. We interpret this behavior by conformations where a number of segments of the chain are adsorbed on one of the four walls and then a number of segments follows which are adsorbed on another of these four walls etc.: only if the chain has wound itself enough along all walls with approximately equal numbers of repeating units adsorbed on each wall $\langle R_{gt}^2\rangle$ will reach its saturation value. This picture of a chain winding itself along the walls of the tube in an irregular screw-like configuration (Fig. 6) also explains why now the longitudinal component (Fig. 3) is distinctly shorter than for the case with no attractive interaction, where the chain is rather nicely stretched out nearly linearly in the center of the tube. In this way we can qualitatively understand the slow crossover in the case $D_T = 4$, $\varepsilon' = -2$ in Fig. 5.

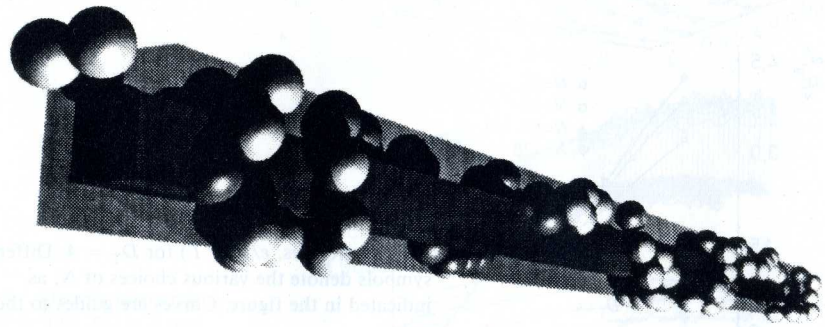

Fig. 6. Snapshot picture of a chain with $N = 128$ repeating units confined in a tube with $D_T = 2$ for strong wall attraction ($\varepsilon/(k_B \cdot T) = -3$). The inner concentric tube with $D_T = 1$ has only been drawn artificially in this figure for the sake of enhancement of the spatial view of the chain and to demonstrate that the chain winds itself around along the walls, it has had no effect in the actual simulation where there was no inner tube present

While with increasing interaction strength $\langle R_{gl}^2\rangle/N$ decreases monotonically for $D_T = 2$ (Fig. 7a), a pronounced minimum is found for $D_T = 4$ (Fig. 7b). In contrast, the behavior of $\langle R_{gt}^2\rangle$ is monotonic for $D_T = 4$ (Fig. 8). Perhaps the interpretation of the minimum in Fig. 7 then is that for $\varepsilon/(k_B \cdot T) = -2$ the chains still have enough room near the walls to take zig-zag-like conformations, while for $\varepsilon/(k_B \cdot T) = -3$ where more repeating units are close to the walls entropy requires the chains to stretch out more. So the minimum could correspond to conformations containing "bridging" of the chain between opposite walls, while for $\varepsilon/(k_B \cdot T) = -3$ these "bridges" have disappeared. A detailed investigation of local structure in the chains is clearly required for full clarification of that point.

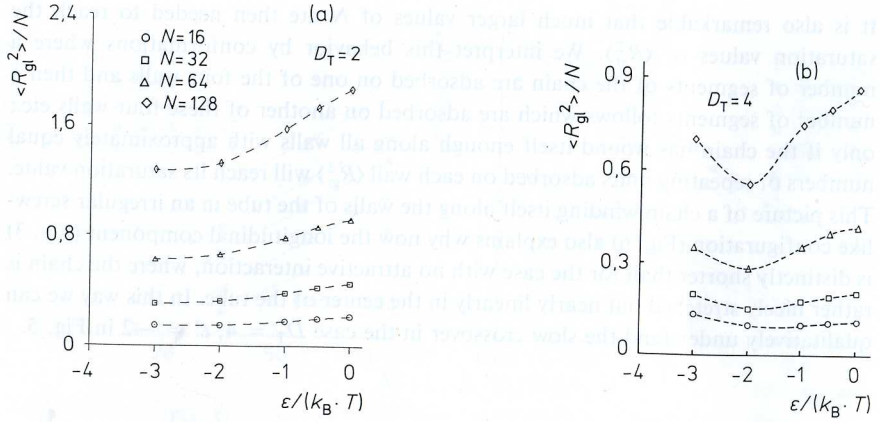

Fig. 7. a) $\langle R_{gl}^2 \rangle / N$ vs. $\varepsilon/(k_B \cdot T)$ for $D_T = 2$. Different symbols denote the various choices of N, as indicated in the figure. Curves are guides to the eye only. b) Same as (a) but for $D_T = 4$

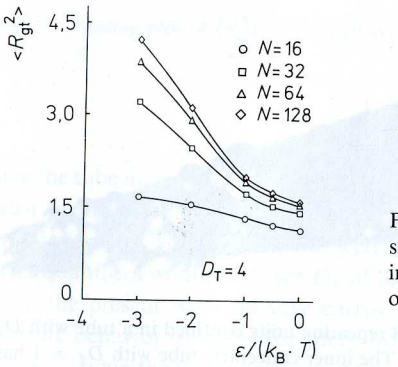

Fig. 8. $\langle R_{gt}^2 \rangle$ vs. $\varepsilon/(k_B \cdot T)$ for $D_T = 4$. Different symbols denote the various choices of N, as indicated in the figure. Curves are guides to the eye only

4. Monomer density profiles in the tube

We have divided the square cross section $D_T \times D_T$ into a fine grid. By counting how often a grid square (centered at x, y) is occupied by the center of gravity of a repeating unit, we obtain a histogram of the repeating unit density $\rho(x, y)$ inside the tube. Since the square symmetry implies that all relevant information is already contained in one quarter $1/2D_T \times 1/2D_T$ of the square, Figs. 9 and 10 display only the histogram of the lower left quarter of the tube in the xy-plane.

As expected, for $\varepsilon' = 0$ the density of repeating units near the walls is zero, and there is a flat maximum in the middle. But already for $\varepsilon' = -0{,}5$ (Fig. 9b) we see a slight but steep increase of the density in the region near the wall. This square-well attractive wall potential then leads to a step in the density near the wall region. While for $\varepsilon' = -1$ and $D_T = 2$ (Fig. 9b) the density maximum in the center of the tube and at the walls are of about equal height, for $\varepsilon' = -2$ (Fig. 9c) the density maximum in the center of the tube has completely disappeared. It can also be clearly recognized that the density near the walls is no constant but gets reduced again near the corners of the

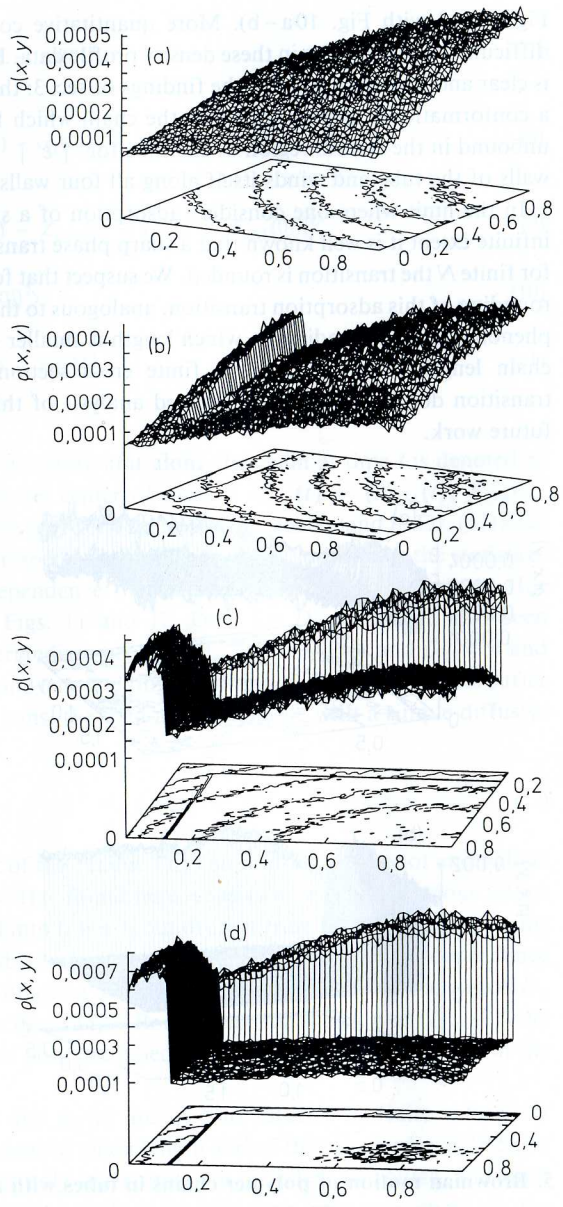

Fig. 9. Density histogram for $N = 128$, $D_T = 2$ and $\varepsilon' = 0$ (a), $-0{,}5$ (b), -1 (c) and -2 (d). Only one quarter of the cross section is shown (x and y run from 0 to $D_T/2 = 1$ as indicated). Note that the z-axis emanates from a corner point of the cross section in (a) and (b), while for clarity of the display the perspective is rotated in (c) and (d), so the z-axis emanates from a mid-point at the boundary of the cross section then

square cross section of the tube. Obviously, it is entropically rather unfavorable for repeating units to get into these edges of the tube, and thus the density reduction near these edges is no surprise. It is also found that different chain lengths do behave extremely similarly, as far as the density profiles for $\varepsilon' = 0$ is concerned, no systematic difference between different choices of N can be detected and also the variation with ε' for different choices of N does not give rise to any remarkable differences (cf.

Fig. 9c–d with Fig. 10a–b). More quantitative conclusions on this problem are difficult due to the noise in these density profile data. However, the general conclusion is clear and in agreement with the findings of sec. 3: the attractive interaction enforces a conformational change such that the chain which for $|\varepsilon'| < 1$ is more or less unbound in the central region of the tube for $|\varepsilon'| \gtrsim 1$ gets strongly bound to the walls of the tube and winds itself along all four walls.

In the limit where one considers adsorption of a single chain on one flat wall of infinite extent it is well known that a sharp phase transition occurs for $N \to \infty$ [5] while for finite N the transition is rounded. We suspect that for finite D there is an additional rounding of this adsorption transition, analogous to the finite-size rounding of critical phenomena [27]. Depending on which length is smaller — $\langle R_{gyr}^2 \rangle_{bulk}^{1/2}$ or D_T — the finite chain length rounding [5] or the finite cross section rounding of the adsorption transition dominates. A more detailed analysis of this situation, however, is left to future work.

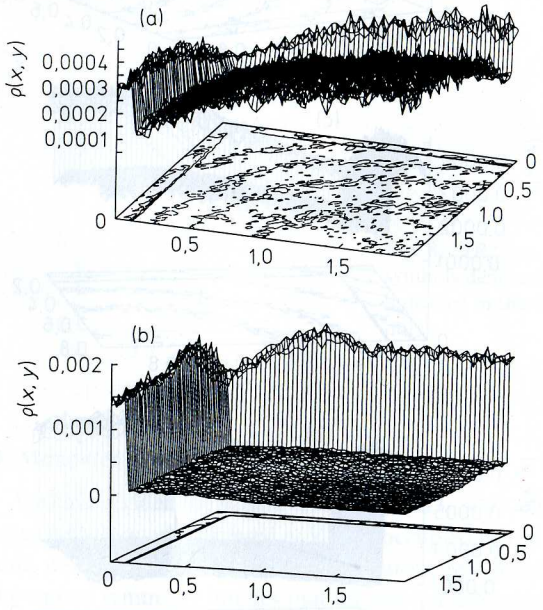

Fig. 10. Same as Fig. 9 but for $D_T = 4$, $N = 32$ and $\varepsilon' = -1$ (a), -2 (b)

5. Brownian motion of polymer chains in tubes with attractive walls

As in our previous work [3, 4, 18, 25] we have found it useful to characterize the motions of the chains in terms of mean-square displacements of both repeating units in the center of the chains and at the chain ends, as well as by their center of mass of motion. Of course, now it is necessary to distinguish between longitudinal displacements (parallel to the tube axis) and transverse ones (perpendicular to the tube axis). Thus the quantities on which we focus attention in the following are defined as (cf. Fig. 1 for a definition of the coordinate axes x, y, z)

$$g_{1l}(t) = \frac{1}{4} \sum_{i=N/2-1}^{N/2+2} \langle [z_i(t) - z_i(0)]^2 \rangle \tag{7}$$

$$g_{1t}(t) = \frac{1}{4} \sum_{i=N/2-1}^{N/2+2} \langle [x_i(t) - x_i(0)]^2 + [y_i(t) - y_i(0)]^2 \rangle \tag{8}$$

$$g_{2l}(t) = \frac{1}{4} \sum_{i=N/2-1}^{N/2+2} \langle [z_i(t) - Z_{CM}(t) - (z_i(0) - Z_{CM}(0))]^2 \rangle \tag{9}$$

$$g_{3l}(t) = \langle [Z_{CM}(t) - Z_{CM}(0)]^2 \rangle \tag{10}$$

$$g_{5l}(t) = \frac{1}{4} \sum_{\substack{i=1,2 \text{ and} \\ N-1,N}} \langle [z_i(t) - z_i(0)]^2 \rangle \tag{11}$$

Here the position of the i'th repeating unit along the chain at time t is denoted as $r_i(t) = (x_i(t), y_i(t), z_i(t))$, and the center of mass is $\boldsymbol{R}_{CM}(t) = (X_{CM}(t), Y_{CM}(t), Z_{CM}(t))$. In Eqs. (7 and 8) we average over 4 units near the center {and in Eq. (11) over 4 units near the two free ends, respectively} simply in order to improve the statistics.

Typical data for the time-dependence of these mean-square displacements (for $\varepsilon/(k_B \cdot T) = 0$) are shown in Figs. 11 and 12. Data for $D_T = 2$ have also been obtained. Their behavior is intermediate between the cases $D_T = 1$ and $D_T = 4$ and they are omitted here. Apart from very late times, where these data sometimes suffer from insufficient length of the runs, the data are compatible with a simple diffusive behavior of the chains,

$$g_{3l}(t) = 2D_N \cdot t \tag{12}$$

D_N being the diffusion constant of the chains. Thus no transient regime of anomalous diffusion $\{g_{3l}(t) \sim t^\alpha$ with $\alpha < 1\}$ is found here, consistent with the previous lattice model study of chains confined into tubes [3], but distinct from the behavior of chains in models for bulk concentrated solutions amd melts [18, 25]. The resulting dependence of the diffusion constant D_N as function of chain length and tube linear dimension D_T is analyzed in Fig. 13. It is seen that simple Rouse behavior is observed ($D_N \sim 1/N$) but the scaling with D_T is rather poor, as expected since D_T is too small to be in the scaling regime (cf. Fig. 4).

The quantities $g_{1t}(t)$, $g_{2l}(t)$ and $g_{5l}(t)$ are seen to saturate at finite values. As expected, $g_{1t}(t \to \infty)$ is independent of chain length and of the same order as $\langle R_{gt}^2 \rangle$. In $\langle R_{gt}^2 \rangle$ all repeating units and not only inner units are included, of course, and since chain ends are more repelled from the walls of the tube than inner monomers are, the behavior of these two quantities is not identical, of course. E. g., for $D_T = 4$ we have $\langle R_{gt}^2 \rangle \approx 1{,}6$ (for $N = 128$) while $g_{1t}(t \to \infty) \approx 2{,}9$. Consistent with this interpretation is the fact that $\langle R_{gt}^2 \rangle$ distinctly increases with increasing N ($\langle R_{gt}^2 \rangle_{N=16} \approx 1{,}43$).

In contrast, both $g_{2l}(t \to \infty)$ and $g_{5l}(t \to \infty)$ have saturation values that increase roughly linear with N (Fig. 14). Of course, since Fig. 3 implies $\langle R_{gl}^2 \rangle \sim N^2$ this result simply says that, due to density fluctuations along the cigar-shaped polymer, the inner unit of the chain makes excursions relative to the center of mass of a relative distance

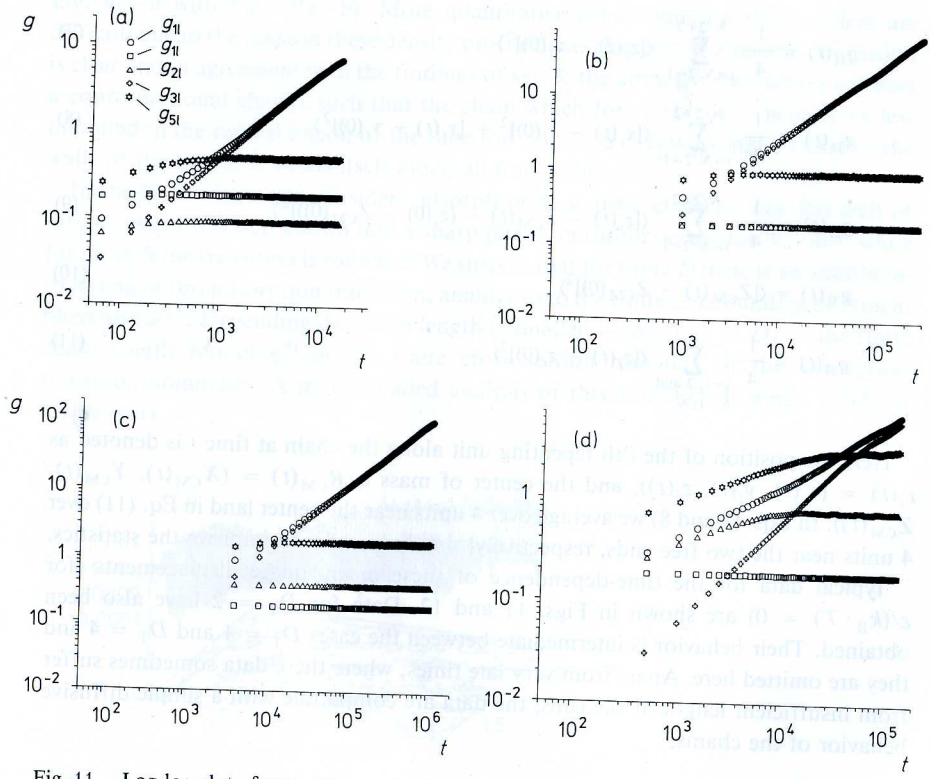

Fig. 11. Log-log plot of mean-square displacements $g_{1l}(t)$, $g_{1t}(t)$, $g_{2l}(t)$, $g_{3l}(t)$ and $g_{5l}(t)$ versus t for $\varepsilon/(k_B \cdot T) = 0$, $D_T = 1$ and chain lengths $N = 16$ (a), 32 (b), 64 (c) and 128 (d). Time t is measured in attempted moves per repeating unit. Different symbols characterize various types of displacements as indicated in the figure.

$|\Delta Z_{CM}|/\sqrt{\langle R_{gl}^2\rangle} \sim 1/\sqrt{N}$, which is expected from Gaussian fluctuations. The mean-square excursions of the ends relative to the center of mass follow the same law but with a larger prefactor.

We now summarize the main predictions of the scaling theory of ref. [3] concerning the dynamic behavior of the displacements, defining a rate W that characterizes the time-dependence of repeating unit displacements in the good-solvent limit. For times $1 \lesssim Wt \lesssim Wt_{tube} \equiv (D_T/\langle l^2\rangle^{1/2})^{2(1+1/(2\nu))}$ one expects Rouse relaxation essentially independent of D_T, i.e.

$$g_{1l}(t) \sim g_{1t}(t) \sim g_{2l}(t) \sim g_{5l}(t) \sim \langle l^2\rangle (WT)^{1/(1+1/(2\nu))} \tag{13}$$

where prefactors of order unity are always omitted. Of course, for the time $t = t_{tube}$ the perpendicular displacement is of the order of D_T, and hence the tube constraint is strongly felt. In fact, inspection of Fig. 12 shows that the time where $g_{1t}(t)$ reaches a plateau is about $t_{tube} \approx 4000$, independent of N. For times $t > t_{tube}$ the

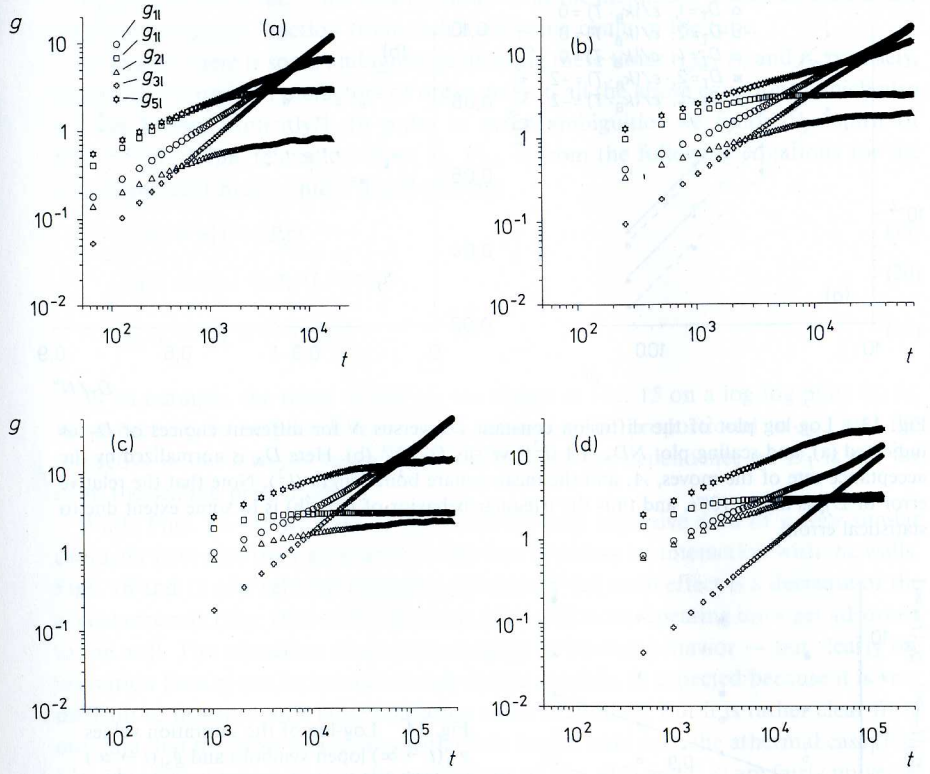

Fig. 12. Same as Fig. 11 but for $D_T = 4$

perpendicular motions are essentially equilibrated and the dynamics is determined by individual motions along the tube. One then expects [3]

$$g_{1l}(t) \sim g_{2l}(t) \sim g_{5l}(t) \sim D_T^2 \cdot (Wt)^{1/2} \cdot (\langle l^2\rangle^{1/2}/D_T)^{(1+1/(2\nu))}$$
$$t_{tube} < t < t_N \tag{14}$$

where the generalized Rouse time t_N,

$$t_N \equiv W^{-1} \cdot (D_T \cdot \langle l^2\rangle^{1/2})^{2-1/\nu} N^2 \tag{15}$$

is the time needed to equilibrate density fluctuations along the chain. It is seen that

$$g_{2l}(t_N) \sim D_T^2 \cdot N \cdot (D_T/\langle l^2\rangle^{1/2})^{1-1/(2\nu)} \cdot (D_T/\langle l^2\rangle^{1/2})^{-1-1/(2\nu)} = D_T^2 \cdot N \cdot \left(\frac{\langle l^2\rangle^{1/2}}{D_T}\right)^{1/\nu}$$

i.e. a mean-square displacement proportional to N (as found in Fig. 14!) is reached. Note also that $g_{2l}(t_N)$ crosses over to the gyration radius square of order $\langle l^2\rangle N^{2\nu}$ of a free chain if the tube gets of this size ($D_T \approx \langle l^2\rangle^{1/2} N^{\nu}$). Of course, this smooth crossover is nothing but a consistency check of the crossover scaling description.

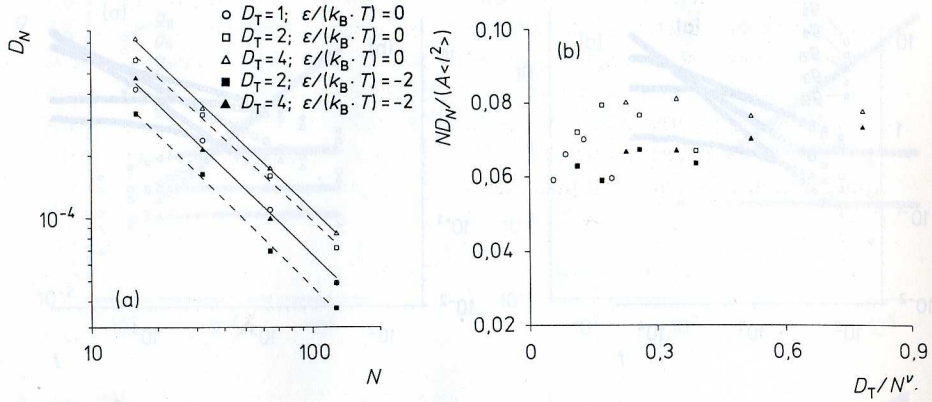

Fig. 13. Log-log plot of the diffusion constant D_N versus N for different choices of D_T as indicated (a), and scaling plot $ND_N/(A\langle l^2\rangle)$ versus D_T/N^{ν} (b). Here D_N is normalized by the acceptance rate of the moves, A, and the mean-square bond length $\langle l^2\rangle$. Note that the relative error of D_N is about 10%, and thus the irregular behavior of part (b) is to some extent due to statistical errors

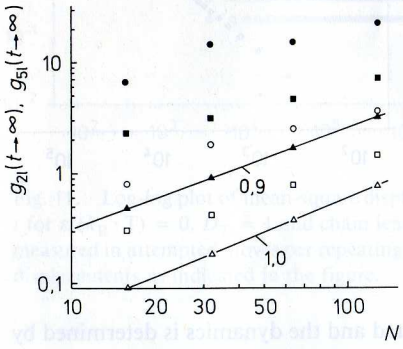

Fig. 14. Log-log of the saturation values $g_{2l}(t\to\infty)$ {open symbols} and $g_{5l}(t\to\infty)$ {full symbols} versus chain length. Straight lines indicate slopes 1,0 and 0,9, respectively. Circles: $D_T = 4$; squares: $D_T = 2$; triangles: $D_T = 1$

For times $t > t_N$, both $g_{2l}(t)$ and $g_{5l}(t)$ have settled down at their respective saturation values, while $g_{1l}(t)$ continues to increase and crosses over to a diffusive behavior,

$$g_{1l}(t) \sim D_N \cdot t \qquad t > t_N \tag{16}$$

From the condition that the crossovers between Eqs. (14) and (16) for $t = t_N$ are smooth one can estimate the chain diffusion constant as

$$D_N \sim W\langle l^2\rangle/N \tag{17}$$

i. e. in the scaling limit D_N should not depend on the tube size D_T. It must be noted, though, that Eq. (15) is not the longest characteristic time of the system: obviously it makes sense to introduce a diffusion time t_D that is needed for a chain to diffuse its own size. Using {cf. Eq. (6)} $\langle R_{gl}^2\rangle \sim \langle l^2\rangle N^2 \cdot (\langle l^2\rangle^{1/2}/D_T)^{2/\nu-2}$ we find

$$t_D \sim D_N^{-1} \cdot \langle R_l^2\rangle = W^{-1} N^3 \cdot (D_T^2/\langle l^2\rangle)^{1-1/\nu} \tag{18}$$

As pointed out in ref. [3] this time t_D shows up as the maximum relaxation time in the coherent scattering function from such a diffusing chain in the tube.

Of course, there is some ambiguity in defining these times t_{tube}, t_N and t_D precisely, in view of the omitted prefactors of order unity in all the above equations (which also are not known explicitly!). In order to avoid ambiguities we follow the spirit of refs. [18, 25] to define relaxation times τ_1^l, τ_{23}^l, τ_3^l from the following equations for the time-dependent mean-square displacements:

$$g_{1l}(t = \tau_1^l) = \langle R_{gl}^2\rangle \tag{19}$$

$$g_{2l}(t = \tau_{23}^l) = g_{3l}(t = \tau_{23}^l) \tag{20}$$

$$g_{3l}(t = \tau_3^l) = \frac{2}{3}\langle R_{gl}^2\rangle \tag{21}$$

As an example, the times τ_3^l and τ_{23}^l are shown in Fig. 15 on a log-log plots vs. N. We expect τ_{23}^l to be proportional to t_N, and τ_3^l to be proportional to t_D, and the respective power laws are indeed nicely seen. Also the dependence on D_T is not far from the scaling prediction.

While Figs. 11–15 all refer to the athermal case, extensive data of a very similar character have also been generated for the case of attractive interaction with the walls. Figs. 16 and 17 give selected examples. Essentially the main effect is a decrease of the acceptance rate (Fig. 16a) of the moves as more and more repeating units get adsorbed to the wall. The relaxation times show roughly Arrhenius behavior — but clearly the relaxation time τ_3^l can be estimated only rather roughly, as expected because it is very difficult to measure such large relaxation times accurately. But it is rather clear from our data that the same power laws with chain length hold as in the athermal case (Fig. 17). This fact emphasizes that the predictions of Eqs. (15) and (18) are fairly universal and independent of details of the model such as the parameter $\varepsilon/(k_B \cdot T)$ — the latter affects only the rate prefactor W^{-1}. Since one could have expected that an adsorbed chain might become essentially immobile and frozen, this is a rather surprising result.

6. Conclusions

In the present work computer simulations have been presented which had the aim to elucidate the static and dynamic behavior of polymer chains confined to narrow pores. We have modelled in a crude way the two principal effects that arise in this situation, in distinction to polymers in solution or melt: *confinement* of polymers due to the restricted geometry inside a tube, and *adsorption* at the walls of the pore due to an attractive interaction between the pore walls and the repeating units forming the chain. In this first exploratory study, we have strongly idealized the situation, by taking the pore strictly straight with constant diameter along the z-direction, disregarding thus both the roughness of the walls of real pores and fluctuations in pore diameter, as well as branching of the pore geometry, etc. It is clear, however, that such complications will arise in reality and deserve separate study. In addition, we have made several crude simplifications which were merely dictated by the need to make our simulation algorithm as fast and efficient as possible: choice of a square rather than circular pore

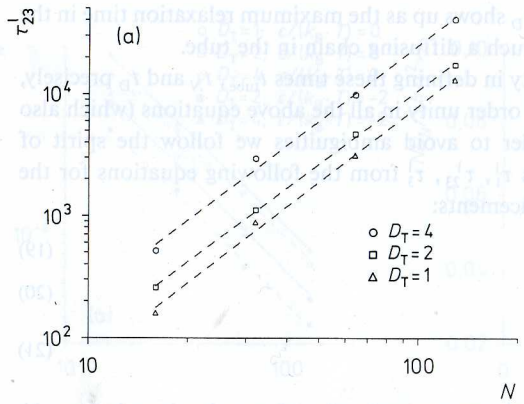

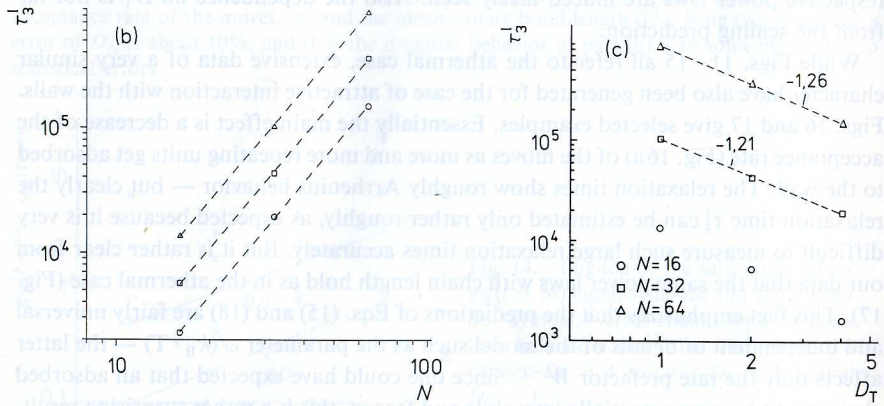

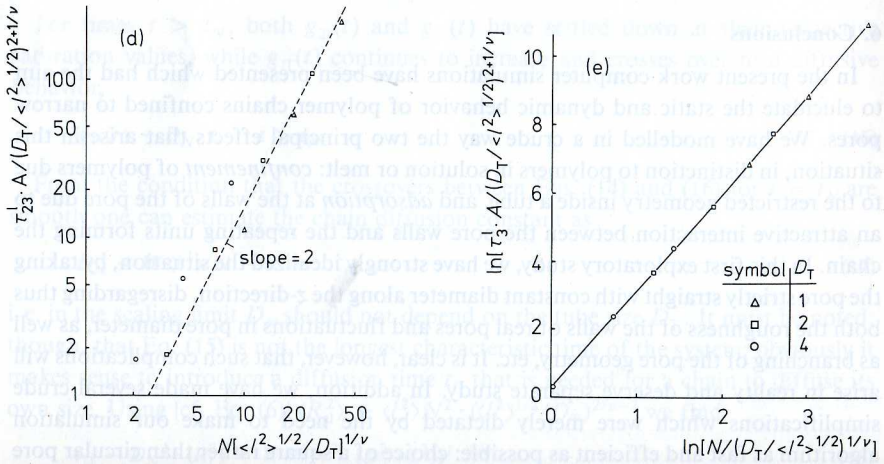

Fig. 15. Log-log plot of the relaxation times τ_{23}^{-1} (a) and τ_3^{-1} (b) versus N, for the athermal case ($\varepsilon/(k_B \cdot T) = 0$) and $D_T = 1$, 2 and 4 as indicated. Straight lines indicate the expected power laws. Part (c) shows a log-log plot of τ_3^{-1} vs. D_T for three choices of N. Straight lines indicate effective exponents (the exponent expected in the scaling limit is $2(1 - 1/\nu) \approx -4/3$. Parts (d) and (e) show scaling plots motivated by Eqs. (15) and (18)

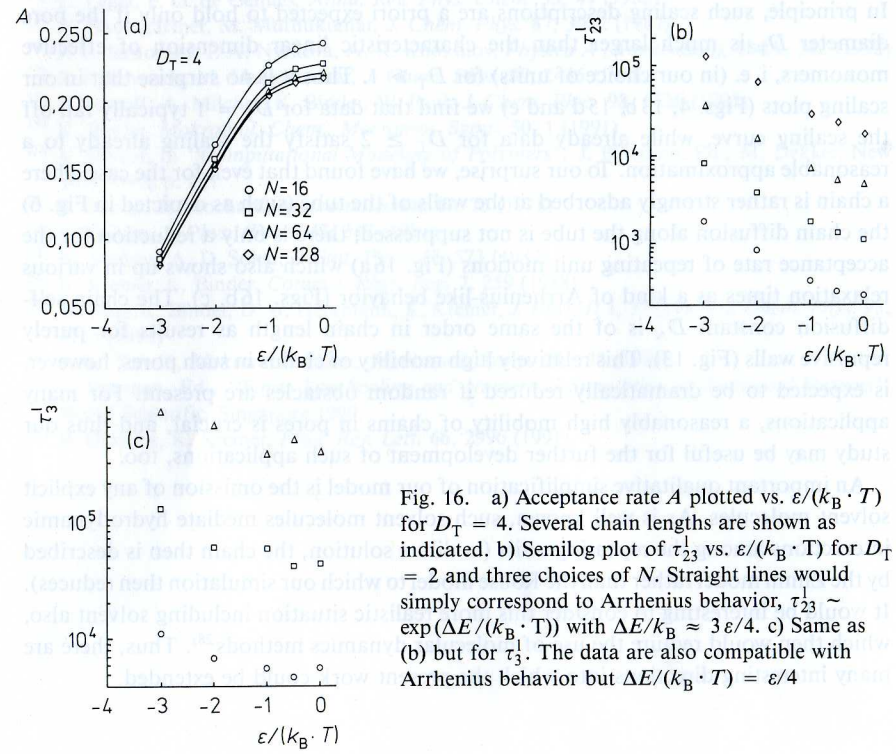

Fig. 16. a) Acceptance rate A plotted vs. $\varepsilon/(k_B \cdot T)$ for $D_T = 4$. Several chain lengths are shown as indicated. b) Semilog plot of τ_{23}^{-1} vs. $\varepsilon/(k_B \cdot T)$ for $D_T = 2$ and three choices of N. Straight lines would simply correspond to Arrhenius behavior, $\tau_{23}^{-1} \sim \exp(\Delta E/(k_B \cdot T))$ with $\Delta E/k_B \approx 3\varepsilon/4$. c) Same as (b) but for τ_3^{-1}. The data are also compatible with Arrhenius behavior but $\Delta E/(k_B \cdot T) = \varepsilon/4$

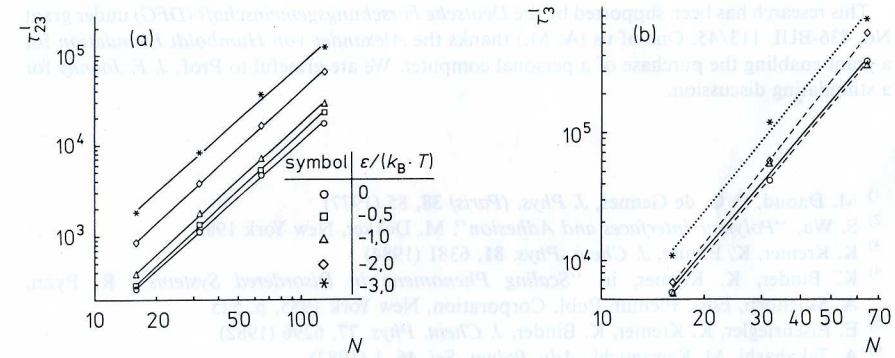

Fig. 17. Log-log plot of the relaxation times τ_{23}^{-1} (a) and τ_3^{-1} (b) versus N for $D_T = 2$ and several choices of $\varepsilon/(k_B \cdot T)$. Straight lines indicate the expected power laws

diameter, choice of a very short square-well potential describing the wall-monomer interaction, and last but not least, choice of a coarse-grained bead-spring type model for the polymer chain. Due to these various simplifying assumptions, our results clearly have a somewhat qualitative character, but they also have a more definite bearing on such aspects of the problem which refer to universal scaling properties of the chains.

In principle, such scaling descriptions are a priori expected to hold only if the pore diameter D_T is much larger than the characteristic linear dimension of effective monomers, i.e. (in our choice of units) for $D_T \gg 1$. Thus it is no surprise that in our scaling plots (Figs. 4, 13b, 15d and e) we find that data for $D_T = 1$ typically fall off the scaling curve, while already data for $D_T \geq 2$ satisfy the scaling already to a reasonable approximation. To our surprise, we have found that even for the case where a chain is rather strongly adsorbed at the walls of the tube (such as depicted in Fig. 6) the chain diffusion along the tube is not suppressed; there is only a reduction for the acceptance rate of repeating unit motions (Fig. 16a) which also shows up in various relaxation times as a kind of Arrhenius-like behavior (Figs. 16b, c). The chain self-diffusion constant D_N is of the same order in chain length as results for purely repulsive walls (Fig. 13). This relatively high mobility of chains in such pores, however, is expected to be dramatically reduced if random obstacles are present. For many applications, a reasonably high mobility of chains in pores is crucial, and thus our study may be useful for the further development of such applications, too.

An important qualitative simplification of our model is the omission of any explicit solvent molecules. As is well known, such solvent molecules mediate hydrodynamic interactions among the repeating units (in dilute solution, the chain then is described by the Zimm model rather than the Rouse model to which our simulation then reduces). It would be interesting to consider this more realistic situation including solvent also, which then would require the use of molecular dynamics methods[28]. Thus, there are many interesting directions into which the present work could be extended.

This research has been supported by the *Deutsche Forschungsgemeinschaft (DFG)* under grant No. 436-BUL 113/45. One of us (A. M.) thanks the *Alexander von Humboldt Foundation* for a grant enabling the purchase of a personal computer. We are grateful to Prof. *J. F. Joanny* for a stimulating discussion.

[1] M. Daoud, P. G. de Gennes, *J. Phys. (Paris)* **38**, 85 (1977)
[2] S. Wu, *"Polymer Interfaces and Adhesion"*, M. Dekker, New York 1982
[3] K. Kremer, K. Binder, *J. Chem. Phys.* **81**, 6381 (1984)
[4] K. Binder, K. Kremer, in *"Scaling Phenomena in Disordered Systems"*, R. Pynn, A. Skjeltorp, Eds., Plenum Publ. Corporation, New York 1985, p. 525
[5] E. Eisenriegler, K. Kremer, K. Binder, *J. Chem. Phys.* **77**, 6296 (1982)
[6] A. Takahashi, M. Kawaguchi, *Adv. Polym. Sci.* **46**, 1 (1982)
[7] P. G. de Gennes, *Adv. Colloid Interface Sci.* **27**, 189 (1987)
[8] W. G. Madden, *J. Chem. Phys.* **87**, 1405 (1987); **88**, 3934 (1988)
[9] S. Lione, H. Meirovitch, *J. Chem. Phys.* **88**, 4498 (1988); H. Meirovitch, S. Lione, *J. Chem. Phys.* **88**, 4507 (1988)
[10] F. van Dieren, K. Kremer, *Europhys. Lett.* **4**, 569 (1987)
[11] M. Doi, S. F. Edwards, *"The Theory of Polymer Dynamics"*, Oxford University Press, Oxford 1986
[12] P. G. de Gennes, *"Scaling Concepts in Polymer Physics"*, Cornell University Press, Ithaca 1979
[13] P. G. de Gennes, *J. Chem. Phys.* **55**, 572 (1971)

[14] L. Leger, P. G. de Gennes, *Annu. Rev. Phys. Chem.* **33**, 49 (1982)
[15] A. Baumgärtner, M. Muthukumar, *J. Chem. Phys.* **87**, 3082 (1987)
[16] F. F. Ternovsky, I. A. Nyrkova, A. R. Khokhlov, *Physica A (Amsterdam)*, **184A**, 342 (1992)
[17] S. F. Edwards, M. Muthukumar, *J. Chem. Phys.* **89**, 2435 (1988)
[18] I. Gerroff, A. Milchev, K. Binder, W. Paul, *J. Chem. Phys.* **98**, 6526 (1993)
[19] K. Binder, *Makromol. Chem., Macromol. Symp.* **50**, 1 (1991)
[20] K. Binder, in *"Computational Modeling of Polymers"*, J. Bicerano, Ed., M. Dekker, New York 1992, p. 221
[21] S. Daoud, F. Brochard, *Macromolecules* **11**, 75 (1978)
[22] L. Turban, *J. Phys. (Paris)* **45**, 347 (1984)
[23] N. Madras, A. D. Sokal, *J. Stat. Phys.* **47**, 573 (1987)
[24] K. Kremer, K. Binder, *Comput. Phys. Rep.* **7**, 259 (1988)
[25] W. Paul, K. Binder, D. W. Heermann, K. Kremer, *J. Phys. II* **1**, 37 (1991); *J. Chem. Phys.* **95**, 7726 (1991)
[26] A. E. Tonelli, *Makromol. Chem., Macromol. Symp.* **65**, 133 (1993)
[27] V. Privman, Ed., *"Finite Size Scaling and Numerical Simulation of Statistical Systems"*, World Scientific, Singapore 1990
[28] B. Dünweg, K. Kremer, *Phys. Rev. Lett.* **66**, 2996 (1991)